PHYSICAL REVIEW D **86,** 083002 (2012)

Revealing cosmic rotation

Amit P. S. Yadav,[1,3] Meir Shimon,[2] and Brian G. Keating[3]

[1]*Institute for Advanced Study, School of Natural Sciences, Einstein Drive, Princeton, New Jersey 08540, USA*
[2]*School of Physics and Astronomy, Tel Aviv University, Tel Aviv 69978, Israel*
[3]*Center for Astrophysics and Space Sciences, University of California, San Diego, 9500 Gilman Drive, La Jolla, California 92093-0424, USA*

(Received 31 July 2012; published 3 October 2012)

Cosmological Birefringence, a rotation of the polarization plane of radiation coming to us from distant astrophysical sources, may reveal parity violation in either the electromagnetic or gravitational sectors of the fundamental interactions in nature. Until only recently this phenomenon could be probed with only radio observations or observations at UV wavelengths. Recently, there is a substantial effort to constrain such nonstandard models using observations of the rotation of the polarization plane of cosmic microwave background (CMB) radiation. This can be done via measurements of the B-modes of the CMB or by measuring its TB and EB correlations which vanish in the standard model. In this paper we show that EB correlations-based estimator is the best for upcoming polarization experiments. The EB-based estimator surpasses other estimators because it has the smallest noise and of all the estimators is least affected by systematics. Current polarimeters are optimized for the detection of B-mode polarization from either primordial gravitational waves or by large-scale structures via gravitational lensing. In the paper we also study the optimization of CMB experiments for the detection of cosmological birefringence, in the presence of instrumental systematics, which by themselves are capable of producing EB correlations, potentially mimicking cosmological birefringence.

DOI: 10.1103/PhysRevD.86.083002 PACS numbers: 98.70.Vc, 98.80.Cq

I. INTRODUCTION

The cosmic microwave background (CMB) is, arguably, the ideal probe of the standard cosmological model. The polarization of the CMB can be studied in terms of the parity-even E-modes and parity-odd B-modes [1–4]. In the standard cosmological model, the physics governing the radiating field is parity invariant. Hence, the parity-odd correlations $\langle TB\rangle$, $\langle EB\rangle$ vanish identically. However, the plane of the CMB's linear polarization can be rotated due to interactions which introduce different dispersion relations for left and right circularly polarized modes, during propagation to us from the last scattering surface. Such rotations generate nonzero $\langle TB\rangle$ and $\langle EB\rangle$ cross-correlations in the CMB. Thus, measurement of these correlations allow estimation of the rotation of the plane of the CMB polarization [5]. Such rotation can come from several processes/sources: e.g., foregrounds, Faraday rotation due to interactions with magnetic fields, and interactions with pseudoscalar fields [6]. The interaction with foregrounds and Faraday rotation lead to frequency-dependent effects; the latter having a frequency dependence ($\propto \nu^{-2}$) [7–10], while interactions with pseudoscalar fields are usually assumed to be frequency independent. The distinct frequency dependencies allow separation of these effects.

We know that parity is violated by weak interactions and is possibly violated in the early universe, giving rise to baryon asymmetry. Hence, investigating the existence of parity violating interactions involving cosmologically evolving scalar fields is well motivated. As an example, an interaction of the form $\frac{\phi}{2M}F_{\mu\nu}\tilde{F}^{\mu\nu}$ [6,11], rotates the polarization plane of linearly polarized light by an angle of rotation $\alpha = \frac{1}{M}\int d\tau\dot{\phi}$ during propagation for a conformal time τ. Here $F_{\mu\nu}$ is the electromagnetic strength tensor, and $\tilde{F}^{\mu\nu}$ is its dual. The fluctuations in the scalar field ϕ are then encoded in the rotation angle α of the polarization.

Faraday rotation, an interaction of CMB with magnetic fields, rotates the plane of polarization by angle $\alpha = \frac{3}{16\pi^2 e}\lambda_0^2\int\dot{\tau}\mathbf{B}\cdot d\mathbf{l}$, where $\dot{\tau} \equiv n_e\sigma_T a$ is the differential optical depth, n_e is the line of sight free electron density, σ_T is the Thomson scattering cross section, a is the scale factor, λ_0 is the observed wavelength of the radiation, $\mathbf{B}$ is the "comoving" magnetic field, and $d\mathbf{l}$ is the comoving length element along the photon trajectory. Magnetic fields are prevalent in cosmic structures at high redshift [12] and it is possible that they may have generated from primordial seed fields imprinted in the early universe (see Ref. [13] for a review). It has been shown that constraining Faraday rotation using the CMB polarization information is a leading diagnostic of a primordial magnetic field [14,15].

As we will show, upcoming CMB polarization probes have the potential to constrain the cosmic birefringence (CB) rotation angle, α, to unprecedented precision–at the $1'$ level. The objective of this paper is to seek optimization schemes for a family of proposed ground-based CMB experiments to detect cosmological birefringence. In particular, we consider the possibility of increasing the size of the observed sky patch at the expense of increasing the map noise of the experiments and explore how this may affect the bounds on CB that these experiments set. We have

considered a range of experiments (varying from Planck-like to cosmic-variance-limited experiment up to $\ell = 3000$) to study general trends.

II. THE CMB AND COSMIC BIREFRINGENCE

In the standard model E and B are pure parity states (even and odd, respectively). The correlation, over the full sky, of the B-mode with either the temperature or E-mode polarization vanishes in this case. However in the presence of CB the polarization plane is rotated, generating $E-B$ mixing which induces "forbidden" TB and EB power spectra. The unrotated CMB temperature field and the Stokes parameters at angular position $\hat{\mathbf{n}}$ are written as $\tilde{T}(\hat{\mathbf{n}})$, and $\tilde{Q}(\hat{\mathbf{n}})$, $\tilde{U}(\hat{\mathbf{n}})$, respectively. The temperature field is invariant under a rotation of the polarization by an angle $\alpha(\hat{\mathbf{n}})$ at the angular position $\hat{\mathbf{n}}$, while the Stokes parameters transform like a spin-2 field:

$$(Q(\hat{\mathbf{n}}) \pm iU(\hat{\mathbf{n}})) = (\tilde{Q}(\hat{\mathbf{n}}) \pm \tilde{U}(\hat{\mathbf{n}}))\exp(\pm 2i\alpha(\hat{\mathbf{n}})). \quad (1)$$

The E and B fields of the CMB are constructed from observed Stokes parameters. In a Fourier basis (in the flat-sky approximation),

$$[E \pm iB](\mathbf{l}) = \int d\hat{\mathbf{n}}[Q(\hat{\mathbf{n}}) \pm iU(\hat{\mathbf{n}})]e^{\mp 2i\varphi_{\mathbf{l}}}e^{-i\mathbf{l}\cdot\hat{\mathbf{n}}}, \quad (2)$$

where $\varphi_{\mathbf{l}} = \cos^{-1}(\hat{\mathbf{n}}\cdot\hat{\mathbf{l}})$. The change in the CMB fields due to rotation is

$$\begin{aligned}
\delta T(\mathbf{l}) &= 0,\\
\delta B(\mathbf{l}) &= 2\int \frac{d^2l'}{(2\pi)^2}[\tilde{E}(\mathbf{l}')\cos 2\varphi_{\mathbf{l}'\mathbf{l}} - \tilde{B}(\mathbf{l}')\sin 2\varphi_{\mathbf{l}'\mathbf{l}}]\alpha(\mathbf{L}),\\
\delta E(\mathbf{l}) &= -2\int \frac{d^2l'}{(2\pi)^2}[\tilde{B}(\mathbf{l}')\cos 2\varphi_{\mathbf{l}'\mathbf{l}} + \tilde{E}(\mathbf{l}')\sin 2\varphi_{\mathbf{l}'\mathbf{l}}]\alpha(\mathbf{L}),
\end{aligned} \quad (3)$$

where $\mathbf{L} = \mathbf{l} - \mathbf{l}'$, and $\varphi_{\mathbf{l}\mathbf{l}'} = \varphi_{\mathbf{l}} - \varphi_{\mathbf{l}'}$. Thus, due to rotation, a mode of wave vector $\mathbf{L}$ mixes the polarization modes of wave vectors $\mathbf{l}$ and $\mathbf{l}' = \mathbf{l}-\mathbf{L}$. Taking the ensemble average of the CMB fields for a fixed α field, for $x \neq x'$ one gets

$$\langle x^{\star}(\mathbf{l})x'(\mathbf{l}')\rangle_{\mathrm{CMB}} = f_{xx'}(\mathbf{l},\mathbf{l}')\alpha(\mathbf{L}), \quad (4)$$

here x, $x' \in \{T, E, B\}$; $f_{TB} = \tilde{C}^{TE}_{l_1}\cos 2\varphi_{\mathbf{l}_1\mathbf{l}_2}$, and $f_{EB} = 2[\tilde{C}^{EE}_{l_1} - \tilde{C}^{BB}_{l_2}]\cos 2\varphi_{\mathbf{l}_1\mathbf{l}_2}$. We have assumed that $\alpha \ll 1$ radian, which is an excellent approximation because current upper limits already set it on the subdegree level [16–18]. The power spectrum is obtained by averaging over many realizations of the CMB, with α fixed. Note that the power spectrum is linearly proportional to α except for $x = x' = B$, where the BB power spectrum is quadratic in α.

If we also average over the rotation field then the above two-point function vanishes for all x, x' except for $x = x'$ for which we are left with the rotation-induced CMB B-mode power spectrum,

$$C^{BB}_L = 4\int \frac{d^2\mathbf{l}'}{(2\pi)^2}C^{\alpha\alpha}_{l'}C^{EE}_{l''}\cos^2[2(\varphi_{\mathbf{l}''} - \varphi_{\mathbf{L}})], \quad (5)$$

where $\mathbf{L} = \mathbf{l}' - \mathbf{l}''$. Note that no assumption has been made here as to the origin of this rotation, namely whether or not it is cosmological. In the literature, α is identified with the CB rotation angle (see Refs. [16,19]).

Constant Rotation Case: For the special case where CB is constant over the sky, i.e., the rotation angle is l-independent:

$$\begin{aligned}
a^{E'}_{\ell m} &= a^{E}_{\ell m}\cos(2\alpha) - a^{B}_{\ell m}\sin(2\alpha),\\
a^{B'}_{\ell m} &= a^{E}_{\ell m}\sin(2\alpha) + a^{B}_{\ell m}\cos(2\alpha),
\end{aligned} \quad (6)$$

and the power spectra become

$$\begin{aligned}
C'^{TB}_{\ell} &= C^{TE}_{\ell}\sin(2\alpha) \quad C'^{EB}_{\ell} = \frac{1}{2}(C^{EE}_{\ell} - C^{BB}_{\ell})\sin(4\alpha)\\
C'^{TE}_{\ell} &= C^{TE}_{\ell}\cos(2\alpha) \quad C'^{EE}_{\ell} = C^{EE}_{\ell}\cos^2(2\alpha) + C^{BB}_{\ell}\sin^2(2\alpha)\\
C'^{BB}_{\ell} &= C^{EE}_{\ell}\sin^2(2\alpha) + C^{BB}_{\ell}\cos^2(2\alpha).
\end{aligned} \quad (7)$$

III. DETECTABILITY OF COSMOLOGICAL BIREFRINGENCE

Following Refs. [20–24], an unbiased quadratic estimator $\hat{\alpha}_{xx'}(\mathbf{L})$ for $\alpha(\mathbf{L})$ for the CMB modes, $xx' = TB$ and EB is

$$\hat{\alpha}_{xx'}(\mathbf{L}) = N_{xx'}(L)\int \frac{d^2l_1}{(2\pi)^2}x(\mathbf{l}_1)x'(\mathbf{l}_2)\frac{f_{xx'}(\mathbf{l}_1,\mathbf{l}_2)}{C^{xx}_{l_1}C^{x'x'}_{l_2}}, \quad (8)$$

where $\mathbf{L} = \mathbf{l}_2 - \mathbf{l}_1$, and the normalization is given by

$$N^{xx'}(L) = \left[\int \frac{d^2l_1}{(2\pi)^2}f_{xx'}(\mathbf{l}_1,\mathbf{l}_2)\frac{f_{xx'}(\mathbf{l}_1,\mathbf{l}_2)}{C^{xx}_{l_1}C^{x'x'}_{l_2}}\right]^{-1}. \quad (9)$$

The fields $x(l)$ can be obtained from the observed map. Here, $C^{xx}_{l_2}$ and $C^{x'x'}_{l_2}$ are the observed power spectra including the effects of both the signal and noise,

$$C^{xx}_{l} = C^{xx,\mathrm{theory}}_{l} + \Delta^2_x e^{l^2\Theta^2_{\mathrm{FWHM}}/(8\ln 2)}, \quad (10)$$

where Δ_x is the detector noise and Θ_{FWHM} is full-width at half-maximum (FWHM) of beamsize.

The variance of the estimator can be calculated as

$$\begin{aligned}
\mathrm{Var}(\tilde{\alpha}(\mathbf{L})) &= \langle\tilde{\alpha}_{xx'}(\mathbf{L})\tilde{\alpha}^{\star}_{xx'}(\mathbf{L}')\rangle\\
&= N^2_{xx'}(L)\int\frac{d^2l_1}{(2\pi)^2}\\
&\quad\times\int\frac{d^2l_3}{(2\pi)^2}\langle x(\mathbf{l}_1)x'(\mathbf{l}_2)x(\mathbf{l}_3)x'(\mathbf{l}_4)\rangle\\
&\quad\times\frac{f_{xx'}(\mathbf{l}_1,\mathbf{l}_2)}{C^{xx}_{l_1}C^{x'x'}_{l_2}}\frac{f_{xx'}(\mathbf{l}_3,\mathbf{l}_4)}{C^{xx}_{l_3}C^{x'x'}_{l_4}},\\
&= (2\pi)^2\delta(\mathbf{L}-\mathbf{L}')\{C^{\alpha\alpha}_L + N_{xx'}(L)\},
\end{aligned} \quad (11)$$

where $\mathbf{L} = \mathbf{l}_2 - \mathbf{l}_1 = \mathbf{l}_4 - \mathbf{l}_3$. In the last line, the first term is the desired CB power spectrum and the second term is the estimator's noise for the reconstruction of CB. The

expression for the noise is given by Eq. (9). The signal-to-noise ratio for detecting CB is given by [21,22]

$$\left(\frac{S}{N}\right)^2 = \sum_2^{l_{\rm max}} \frac{f_{\rm sky}}{2}(2l+1)\left(\frac{C_l^{\alpha\alpha}}{N_l^{xx'}}\right)^2, \qquad (12)$$

where $C_L^{\alpha\alpha}$ is the fiducial rotation angle power spectrum.

In Fig. 1, we show the quadratic EB estimator noise as a function of multipole, ℓ, for four experimental configurations. For reference we show two theoretical Faraday rotation power spectra (black solid curves), one which corresponds to the scale-invariant magnetic field spectrum and the other for the model with a causal stochastic magnetic field. Details on these models involving Faraday rotation can be found in Ref. [15]. For the experiments considered here, the EB-estimator is the most sensitive, as will be demonstrated.

A Constant Rotation Case: For uniform rotation, $\mathbf{L} = \mathbf{l}_1 - \mathbf{l}_2 = 0$ in Eq. (9), hence there is no mode mixing between different wave vectors. Although we do not show the "monopole term," $L = 0$, in Fig. 1, the estimator can also be used to find the detectability of uniform rotation. The signal-to-noise (S/N) for the detection of non-vanishing C_l^{EB} is

$$(S/N)^2_{EB} = \sum_l f_{\rm sky}\frac{(2l+1)}{2}\frac{(C_l^{EB,obs})^2}{C_l^E C_l^B}. \qquad (13)$$

The power spectrum in the numerator, $C_l^{EB,obs}$, is the observed spectrum, and the power spectra C_l^{EE} and C_l^{BB} in the denominator include the effects of noise and beam smearing [see Eq. (10)]. Similar expressions can be written for $(S/N)_{TB}$ by replacing E by T. Note that for a cosmic-variance-limited experiment, $(S/N)_{EB}$ will exceed $(S/N)_{TB}$ because the cosmic variance of the temperature anisotropy is at least an order of magnitude larger than that of the E-mode polarization.

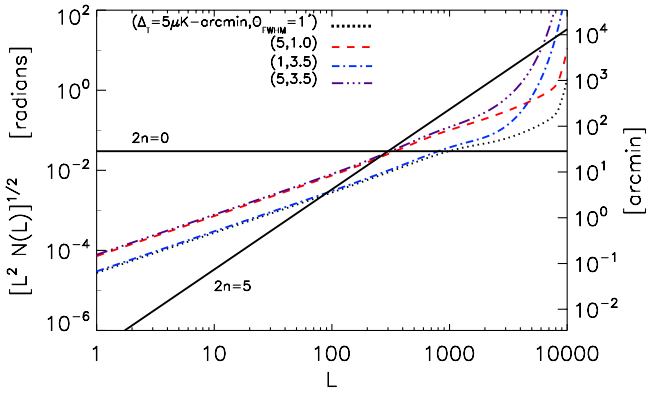

FIG. 1 (color online). Detectability of CB using the EB estimator. We show the EB estimator noise, $N(L)$, as given by Eq. (9), as a function of multipole L. We show the noise for four experimental setups. The noise, Δ_T in μK − arcmin and beam full-width at half-maximum $\Theta_{\rm FWHM}$–units of arcmin, is labeled. For reference, the two solid curves (black) show the Faraday rotation power spectrum from the stochastic magnetic field with "causal spectrum" ($2n = 5.0$) and for a nearly scale-invariant spectrum ($2n = 0.1$).

Employing the conventional definition of the Fisher matrix, and assuming constraints from the EB data, we obtain

$$F_{ij}^{EB} = \sum_l f_{\rm sky}\frac{(2l+1)}{2}\frac{\partial(C_l^{lEB})}{\partial\lambda_i}\frac{\partial(C_l^{lEB})}{\partial\lambda_j}(C_l^B C_l^E)^{-1}, \qquad (14)$$

and the error on the parameter λ_i is given by $\sigma_i = \sqrt{[(F^{EB})^{-1}]_{ii}}$, the i'th diagonal element of the square root of the inverse Fisher matrix. In the simplest case we consider, there is only a single parameter, the rotation angle α, and the calculation is trivial. A similar expression can be written for the TB estimator. It should be noted that assuming small instrumental noise, such as EPIC [25], CMBPol [26–28], and COrE [29] the EB estimator outperforms the TB estimator. This can be readily seen from the fact that $\sqrt{C_l^T C_l^E} \geq C_l^{TE}$, is the Cauchy-Schwarz inequality. In the other extreme, when the experiment is dominated by instrument noise, the TB estimator performs the best. This is due to the fact that $C_l^{TE} > C_l^{EE}$ and the fact that $C_l^{E,\rm det} = 2C_l^{T,\rm det}$. This result is also clear from Fig. 2 where we compare the EB and TB estimators of various noise configurations.

Optimizing surveys for CB detection can be approached as follows: given the detector noise Δ_0 for an experimental setup, we can get $\Delta = \Delta_0(\frac{f_{\rm sky}}{f^0_{\rm sky}})^{1/2}$. Here $f^0_{\rm sky}$ is a fiducial sky-fraction. Note that larger the $f_{\rm sky}$, the shorter the observation time in a given sky direction, making the noise, Δ, correspondingly higher. In Fig. 3 we show how changing the sky-fraction, $f_{\rm sky}$ changes the performance of the EB estimator. In general

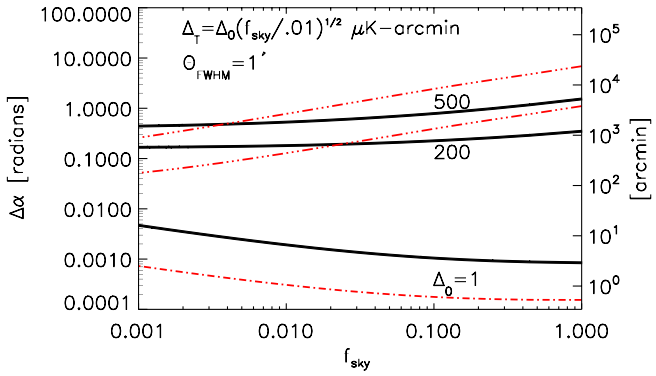

FIG. 2 (color online). Comparison of the EB and TB estimator for constant α case. We show forecasted uncertainties on constant α from the two estimators as a function of sky-fraction $f_{\rm sky}$, for several choices of instrumental noise. The dashed-dotted curves (red) are for the EB estimator while the solid curves (black) are for the TB estimator. Clearly the EB estimator outperforms the TB estimator for the experiments with low enough noise such as EBEX [40], CMBPol [26], POLARBEAR [31], SPTPol [41], and SPIDER [42]. Note that for a given observing time, the noise Δ_T is proportional to $\sqrt{f_{\rm sky}}$ and hence can be reduced by observing smaller sky-fractions.

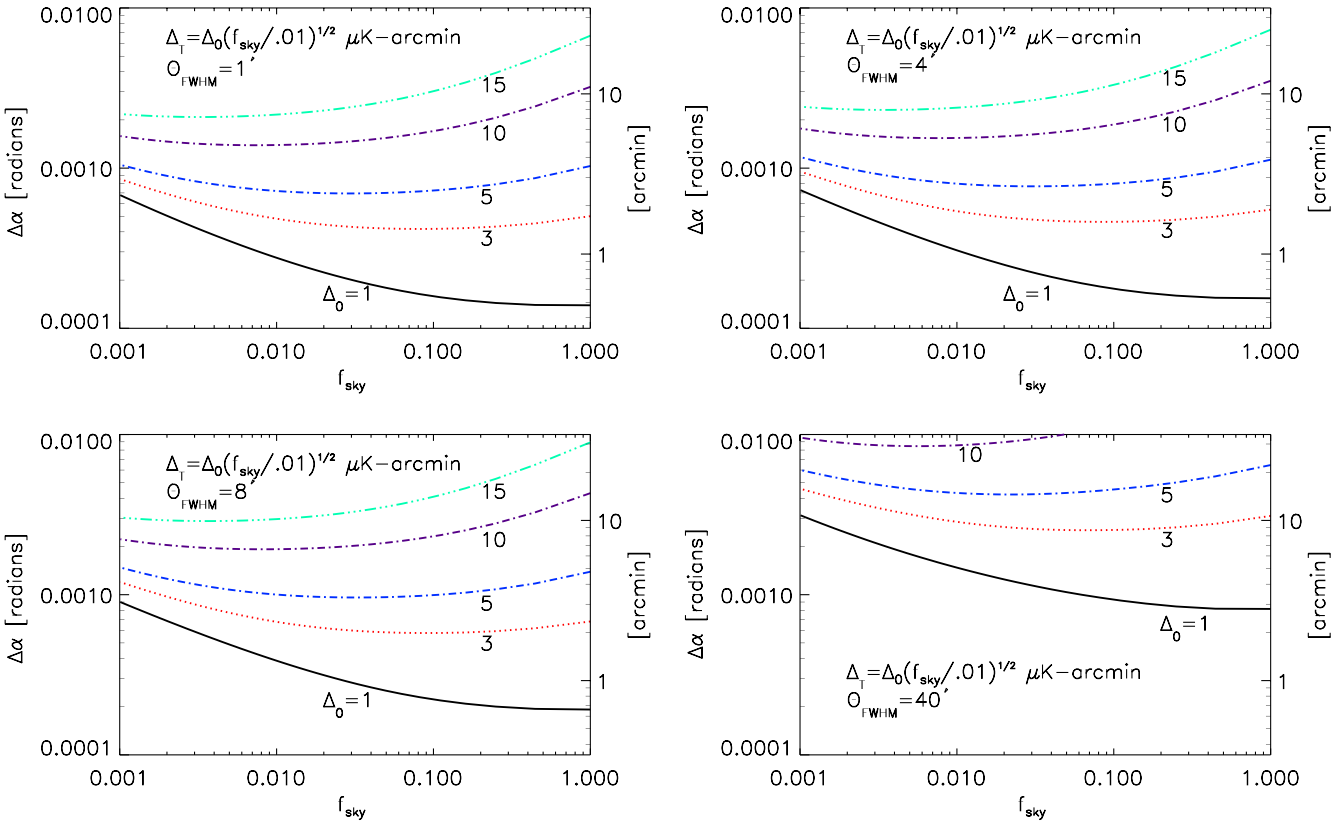

FIG. 3 (color online). Forecasted uncertainties on constant α from the EB estimator as a function of sky-fraction $f_{\rm sky}$, for several choices of instrumental noise. The minima for the curves are a result of compromise between number of modes and noise Δ_p. Note that the observing time was fixed.

there is a preferred $f_{\rm sky}$ for which the error in CB is minimized. For the noise-dominated experiment it is preferred to have lower $f_{\rm sky}$. For a nearly cosmic-variance-limited experiment it is always favorable to have larger $f_{\rm sky}$. We discuss the physical reasons for this behavior in our results section.

IV. REQUIREMENT ON INSTRUMENTAL SYSTEMATICS

So far the CB detection prospects in the absence of systematics have been discussed. It has been shown that there are several instrumental systematics that can generate EB and TB correlations which also generate spurious B-mode polarization [24,30]. Although the CMB experiments considered in this paper were designed to detect the very weak B-mode signal from inflationary gravitational waves [26,31], it has been shown [30] that this feature of these CMB experiments may be insufficient for an unbiased detection of CB.

Polarimeters such as *MaxiPol* [32], *Boomerang* [33], *BICEP* [34], *QUAD* [35] etc., detect the difference in intensity from bolometers sensitive to two orthogonal polarizations. Any differences between the two bolometers generate spurious Q and U signals. Furthermore, the spatial beams that each bolometer produces generally have some degree of ellipticity. Following the formalism presented in Ref. [36], polarization systematics fall into two categories, one associated with the detector system which distorts the polarization state of the incoming polarized signal (hereafter "Type I"), and another associated with systematics of the CMB signal due to the beam anisotropy ("Type II"). To first order, the effect of Type I systematics on the Stokes parameters can be written as [36]

$$\begin{aligned}\delta[Q \pm iU](\hat{\mathbf{n}}) = {} & [a \pm i2\omega](\hat{\mathbf{n}})[Q \pm iU](\hat{\mathbf{n}}) \\ & + [f_1 \pm if_2](\hat{\mathbf{n}})[Q \mp iU](\hat{\mathbf{n}}) \\ & + [\gamma_1 \pm i\gamma_2](\hat{\mathbf{n}})T(\hat{\mathbf{n}}),\end{aligned} \tag{15}$$

where $a(\hat{\mathbf{n}})$ is a scalar field which describes the polarization miscalibration, $\omega(\hat{\mathbf{n}})$ is a scalar field that describes the rotation misalignment of the instrument, $(f_1 \pm if_2)(\hat{\mathbf{n}})$ are spin ± 4 fields that describe the coupling between two spin ± 2 states (spin-flip), and $(\gamma_1 \pm i\gamma_2)(\hat{\mathbf{n}})$ are spin ± 2 fields that describe monopole leakage, i.e., leakage from CMB temperature anisotropy to polarization.

Similar to the Type I systematics, the effect of Type II systematics on the Stokes parameters can be written as [36]

$$\begin{aligned}\delta[Q \pm iU](\hat{\mathbf{n}};\sigma) = {} & \sigma\mathbf{p}(\hat{\mathbf{n}}) \cdot \nabla[Q \pm iU](\hat{\mathbf{n}};\sigma) \\ & + \sigma[d_1 \pm id_2](\hat{\mathbf{n}})[\partial_1 \pm i\partial_2]T(\hat{\mathbf{n}};\sigma) \\ & + \sigma^2 q(\hat{\mathbf{n}})[\partial_1 \pm i\partial_2]^2 T(\hat{\mathbf{n}};\sigma),\end{aligned} \tag{16}$$

where the systematic fields are smoothed over the coherence size σ. The spin ± 1 fields, $(p_1 \pm ip_2)$ and $(d_1 \pm id_2)$, describe pointing errors and dipole leakage from temperature to polarization, respectively, and q is a scalar field that represents quadrupole leakage [36], e.g., beam ellipticity.

We now discuss how systematics contaminate the rotation estimator. We start by defining a matrix $F_\ell^{\alpha\mathcal{D}'}$ for each multipole ℓ,

$$F_\ell^{\alpha\mathcal{D}'} = \int \frac{d^2 l_1}{(2\pi)^2} f_{EB}^{\alpha}(\ell_1, \ell_2)(\mathbf{C}^{-1})_{\ell_1}^{EE} f_{EB}^{\mathcal{D}}(\ell_1, \ell_2)(\mathbf{C}^{-1})_{\ell_2}^{BB}, \tag{17}$$

where $\ell = \ell_1 - \ell_2$, and $\mathcal{D}$ run over all the 11 systematics and lensing, $\{a, \omega, \gamma_1, \gamma_2, f_1, f_2, d_1, d_2, q, p_1, p_2, \phi\}$. The filters $f^{\mathcal{D}}(\ell_1, \ell_2)$ are given in Refs. [24,36]. Our estimator, in the absence of any distorting systematics field, is unbiased, meaning that

$$\langle \hat{\alpha}(\mathbf{L}) \rangle_{\rm CMB} = \alpha(\mathbf{L}). \tag{18}$$

However, in the presence of multiple systematic effects the estimator as constructed in Eq. (8) may not be unbiased. In general Eq. (18) is modified as

$$\langle \hat{\alpha}(L) \rangle_{\rm CMB} = \alpha(L) + \frac{\sum_{\mathcal{D}} F_L^{\alpha\mathcal{D}} \mathcal{D}'(L)}{F_L^{\alpha\alpha}}, \tag{19}$$

where $\hat{\alpha}$ is an estimate of α in the presence of multiple systematics. The level of bias depends on the Fisher matrix, $F_L^{\alpha\mathcal{D}}$, and the amplitude of systematics, $\mathcal{D}$.

Systematics induced B-mode power spectrum is given by

$$\langle B(\mathbf{l}_1) B(\mathbf{l}_2) \rangle_{{\rm CMB},\mathcal{D}} = (2\pi)^2 \delta(\mathbf{l}_1 + \mathbf{l}_2) \int \frac{d^2 \mathbf{l}'}{(2\pi)^2} C_{l'}^{\mathcal{D}\mathcal{D}} \tilde{C}_{l''}^{xx} W_{\mathcal{D}}^{B}(\mathbf{l}', \mathbf{l}'') W_{\mathcal{D}}^{B}(\mathbf{l}', \mathbf{l}''), \tag{20}$$

where $\mathbf{l}'' = \mathbf{l}_1 - \mathbf{l}'$; $x = E$ for systematics with E to B leakage, $(\mathcal{D} = a, \omega, (f_1, f_2), (p_1, p_2))$; and $x = T$ for systematics with T to B leakage $[\mathcal{D} = q, \omega, (\gamma_1, \gamma_2), (d_1, d_2)]$. We have assumed zero primordial B-modes for our fiducial model. The window function, $W_{\mathcal{D}}^{B}(\mathbf{l}_1, \mathbf{l}_2)$, for each of the systematics, $\mathcal{D}$, are given in Refs. [24,36].

In Table I we compare the requirement on instrumental systematics for the measurement of CB either via the B-modes or by using the EB estimator. In the table, the first column lists the systematics considered. In columns 2–5 we show the requirement from rotation induced B-mode power spectrum. This requirement was derived by demanding that the systematics induced B-mode power spectrum [as given by Eq. (20)] is 10 times smaller than the rotation induced B-mode power spectrum detectable by that experimental setup. Columns 6–9 give the minimum *rms* level of each systematics $\mathcal{D}$ such that the bias generated by that systematic for CB estimation is 10 times smaller than the rotation field. To be more precise, we require that the underlying CB power spectrum $C_\ell^{\alpha\alpha}$ is 10 times smaller than the bias contribution to the power spectrum arising from second term on the right-hand side of Eq. (19). We used $L = 100$ for this requirement however the requirement for $L = 0$ (the monopole, or constant

TABLE I. Requirement on instrumental systematics for the measurement of cosmic birefringence. The first column lists the systematics considered while remaining columns show the minimum-systematics *rms* requirement for different experimental setups (E1–E4). Experimental noise Δ_T in μK − arcmin and beam full-width at half-maximum, $\Theta_{\rm FWHM}$, for each experiment is provided in the round brackets. In columns 2–5 we show the requirement from rotation-induced B-mode power spectrum. This requirement was derived by demanding that the systematics-induced B-mode power spectrum is 10 times smaller than the rotation-induced B-mode power spectrum detectable by that experimental setup. Columns 6–9 show the requirement for the EB quadratic estimator. This requirement was derived using Eq. (19), where we demand that the spurious power-spectrum contamination to the rotation EB estimator [coming from the second term at the right-hand side of Eq. (19)] is 10 times smaller than the fiducial underlying the rotation power spectrum.

	Requirement							
	B-mode Spectrum				EB Estimator			
Systematics	E1 ($\Delta_T = 1', 1$)	E2 (5, 1′)	E3 (1, 3.5′)	E4 (5, 3.5′)	E1 (1, 1′)	E2 (5, 1′)	E3 (1, 3.5′)	E4 (5, 3.5′)
a	1.1×10^{-3}	2.8×10^{-3}	1.2×10^{-3}	3.1×10^{-3}	···	···	···	···
γ_1	1.1×10^{-5}	2.7×10^{-5}	1.1×10^{-5}	3.0×10^{-5}	···	···	···	···
γ_2	8.6×10^{-6}	2.2×10^{-5}	9.4×10^{-6}	2.5×10^{-5}	0.10	0.08	0.1	0.08
f_1	1.1×10^{-3}	2.9×10^{-3}	1.2×10^{-3}	3.2×10^{-3}	···	···	···	···
f_2	1.0×10^{-3}	2.6×10^{-3}	$1.1 \times 1o^{-3}$	2.9×10^{-3}	···	···	···	···
d_1	1.2×10^{-4}	3.2×10^{-4}	7.1×10^{-5}	1.8×10^{-4}	0.1	0.56	0.04	0.24
d_2	1.3×10^{-4}	3.5×10^{-4}	7.8×10^{-5}	2.0×10^{-4}	···	···	···	···
q	1.4×10^{-3}	3.6×10^{-3}	4.3×10^{-4}	1.1×10^{-3}	···	···	···	···
p_1	2.0×10^{-2}	5.3×10^{-2}	1.2×10^{-2}	3.06×10^{-2}	0.16	0.4	0.05	0.13
p_2	1.2×10^{-2}	3.3×10^{-2}	7.3×10^{-3}	1.9×10^{-2}	···	···	···	···

TABLE II. Projected constraints from various experimental configurations on the constant cosmic rotation α. Experimental specifications are shown in columns 1–3. Columns 4–7 show the expected uncertainties on α from both the TB and EB estimators, without and with systematics marginalized. It is clear that the EB estimator yields tighter constraints on α.

Δ_T [μK − arcmin]	$f_{\rm sky}$	$\Theta_{\rm FWHM}$ [arcmin]	$\Delta\alpha_{TB}$ [rad]	$\Delta\alpha_{TB+{\rm sys}}$ [rad]	$\Delta\alpha_{EB}$ [rad]	$\Delta\alpha_{EB+{\rm sys}}$ [rad]
1.0	0.1	1.0	0.27E-3	0.30E-3	0.87E-4	0.10E-3
5.0	0.1	1.0	0.66E-3	0.69E-3	0.22E-3	0.25E-3
5.0	0.1	3.5	0.71E-3	0.74E-3	0.24E-3	0.28E-3
1.0	0.1	3.5	0.29E-3	0.32E-3	0.94E-4	0.11E-3
1.0	0.01	1.0	0.88E-3	0.96E-3	0.27E-3	0.32E-3
5.0	0.01	1.0	0.21E-2	0.22E-2	0.72E-3	0.82E-3
1.0	0.01	3.5	0.95E-3	0.10E-2	0.30E-3	0.35E-3
5.0	0.01	3.5	0.23E-2	0.24E-2	0.79E-3	0.91E-3

rotation case) is comparable. We show the numbers for several experimental configurations. Note that the systematics fields a, γ_1, f_1, f_2, d_2, q and p_2 are uncorrelated with rotation α and hence do not bias the estimator. For the remaining systematic fields γ_2, d_1 and p_1 the requirement is not particularly stringent when compared to the requirement for extracting the rotation from the B-mode power spectrum. The *rms* requirement on the systematics depends on the experimental configuration and for experiments in consideration in Table I. Even the most stringent requirement is around 5%, which is easily achievable with current experiment designs. We note that for the simple frequency-independent model shown earlier, constant CB is completely degenerate with the differential rotation beam systematic ω [30]. Therefore measuring anisotropic $\alpha(\hat{\mathbf{n}})$ [37] is *less sensitive* to systematics contamination.

Throughout our analysis we have assumed systematics to be isotropic Gaussian fields with power spectra of the form

$$C_l^{\mathcal{D}\mathcal{D}} = A_{\mathcal{D}}^2 \exp(-l(l+1)\sigma_{\mathcal{D}}^2/8\ln 2), \qquad (21)$$

i.e., white noise above a certain coherence scale $\sigma_{\mathcal{D}}$. The parameter $A_{\mathcal{D}}$ characterizes the *rms* of the systematics field $\mathcal{D}$. For our numerical calculations we have assumed $\sigma_{\mathcal{D}} = 120'$.

Beam Systematics for a Constant CB Case: We discussed the requirements on systematics, however we can marginalize over unknown beam parameters. This is possible due to the fact that e.g., beam ellipticity and beam offset have different L-dependence than CB and can therefore be distinguished from a pure CB. In other words, the Fisher matrix is regular and invertible. However, pixel rotation is completely degenerate with α and we therefore can offer no method of disentangling it from the measured α other than a precise calibration with polarized sources [38]. It turns out that including the beam ellipticity and beam offset effects in our Fisher matrix estimation is surprisingly easy. The analytic model for beam systematics considered by Ref. [39] gives the systematic TB and EB spectra from the combined effect of beam offset ρ and ellipticity e

$$C_\ell^{TB,{\rm sys}} = A_1 l^2 C_\ell^{TT}, \qquad C_\ell^{EB,{\rm sys}} = A_2 l^4 C_\ell^{TT}, \qquad (22)$$

where the two new free parameters A_1 and A_2 are certain combinations of e and ρ. The Fisher matrices in Eq. (14) now become two-dimensional. In Table II we show 1σ error on constant CB, α from the EB and the TB estimator with and without the systematics parameters marginalized. It is clear from Table I that for various experimental configurations, the systematics increases the error by only 10%–20%.

V. RESULTS AND DISCUSSION

In Fig. 1 we show the minimum detectable spatially dependent CB. We show the EB quadratic estimator noise as a function of multipole L for several experimental configurations. For a given multipole L, the noise level sets the minimum detectable signal for that multipole. For reference we have also shown two fiducial theoretical Faraday rotation power-spectra, for a scale-invariant and causal stochastic magnetic field [15]. It is clear from the plot that for scale invariant case largest contribution to the (S/N) comes from large-scale (low L), while for causal magnetic fields, small scales (large L) contribute the most.

In Fig. 2 we compare the TB and EB estimator for the constant CB case. It is clearly seen that the EB estimator results in better constraints on α for current and future polarization experiments. We also show curves for relatively large experimental noise cases $\Delta_T = 200,\ 500\ \mu$K − arcmin to show that, for experiments with larger noise levels, the TB estimator performs better.

In Fig. 3 we study the optimization of polarization experiments seeking to constrain CB. We show the minimum detectable rotation angle as a function of the sky-fraction, $f_{\rm sky}$, for several choices of instrument detector sensitivity. Here the observing time was fixed. For smaller $f_{\rm sky}$ the noise will be lower but at the cost of smaller number of modes. While if $f_{\rm sky}$ is large, we will have more modes at the cost of larger noise. This compromise between the number of modes and noise is visible in the plot in the form of preferred minima in the curve $\Delta\alpha$-versus-$f_{\rm sky}$.

In Table I we study the requirements on instrumental systematics to be able to utilize a given experiment for detecting or constraining CB. Here we have considered 11

systematics. For each systematic we ask, how small their *rms* fluctuation must be such that they do not affect detection of CB using (1) the B-mode power spectrum (2) EB estimator. The conclusion of this analysis tells that EB estimator is much less prone to instrumental systematics, i.e., the requirement on EB systematics effects are much weaker than for the B-mode spectra. In fact there are several systematics (a, γ_1, f_1, f_2, d_2, q and p_2) which do not affect the estimation of rotation with EB estimator while all the systematics affect the estimation using the B-mode spectrum. Even for the systematics which do affect EB estimator, the requirements on systematics *rms* control is three orders of magnitude smaller than the corresponding requirement from B-modes. We also note that lensing deflection is same as the pointing systematics parameter p_2. We show in Table I that p_2 is orthogonal to CB and does not bias the CB estimator. Hence lensing also does not bias the CB estimator.

In Table II, we give our forecasted Fisher uncertainties on constant CB α. The experimental configurations used to get the constraints are also shown in the first three columns. It is seen from the Table II that the EB estimator gives constraints $\sim$3 times better than those obtained from employing the TB estimator. This is due to the fact that the experiments considered here are near cosmic-variance-limited and that C_l^{TT} is $\sim$10 times larger than C_l^{EE} on the range of multipoles considered ($l_{\rm max} = 3000$ in our calculation). It is also apparent from Table II that adding in the beam systematics does not degrade our constraints by more than 20% due to the fact the beam-systematics-induced TB and EB are only weakly degenerate with pure CB (different L-dependence and the fact that the experiments we consider cover a sufficiently wide multipole range to allow separation of systematic TB and EB from cosmological birefringence). One could add additional free parameters but our results are not expected to significantly change because the L-dependence is different enough to allow separation between CB and beam systematic effects.

VI. CONCLUSIONS

Any mechanism capable of converting E- to B-mode polarization will necessarily leak the TE and EE correlations to TB and EB, respectively. Nonvanishing TB and EB could be used, for example, to monitor residual systematics during data processing [24,30], to constrain Faraday rotation, or to constrain parity violating physics. In this paper we presented a simple analytic approach to the optimization of ground-based CMB polarization observations capable of CB detection. We studied and compared the detection capabilities using the EB correlations, TB correlations, and the B-mode power spectrum. We find the EB correlation based estimator to be the best, both in terms of having the least noise and also suffering the least from systematic effects. Special care should be given to systematics because they can generate spurious EB correlations in the CMB–widely considered as a smoking gun for CB. We demonstrated that this is probably not a significant issue when one performs a global parameter estimation, leaving beam parameters as nuisance parameters in the analysis. We find that in general there is a preferred sky-fraction $f_{\rm sky}$ for which the errors on CB are minimized. However for experiment with noise $<5\ \mu{\rm K} - {\rm arcmin}$, a very deep observing mode will result in weaker constraints on CB and that increasing the observed sky area typically exhausts the capacity to constrain CB. However, adopting such a wide sky coverage will come at the expense of the very high sensitivity required for the inflation-induced B-mode–the tradeoff between these two scientific goals is clear and in order to optimize future experiments it is desirable to define a metric for the successful measurement of both signals. Complications from astrophysical foregrounds were not considered in this paper. It is our hope that future CMB observations will provide crucial information of the emission mechanisms that could produce spurious TB and EB correlations in the CMB. In any case, these foregrounds have very different spectral radiance behaviors than the CMB and so by using multi-frequency observations one may hope to remove their contribution, at least in part. In addition, their spatial profile and possibly their clustering properties could be used to further identify these noncosmological contributions and separate them out from the data.

ACKNOWLEDGMENTS

A. P. S. Y. acknowledges support from NASA Grant No. NNX08AG40G. M. S. was supported by the James B. Ax Family Foundation.

[1] U. Seljak and M. Zaldarriaga, Phys. Rev. Lett. **78**, 2054 (1997).
[2] U. Seljak and M. Zaldarriaga, astro-ph/9805010.
[3] M. Kamionkowski, A. Kosowsky, and A. Stebbins, Phys. Rev. D **55**, 7368 (1997).
[4] M. Kamionkowski, A. Kosowsky, and A. Stebbins, Phys. Rev. Lett. **78**, 2058 (1997).
[5] A. Lue, L. Wang, and M. Kamionkowski, Phys. Rev. Lett. **83**, 1506 (1999).
[6] S. M. Carroll, Phys. Rev. Lett. **81**, 3067 (1998).
[7] A. Kosowsky and A. Loeb, Astrophys. J. **469**, 1 (1996).
[8] A. Kosowsky, T. Kahniashvili, G. Lavrelashvili, and B. Ratra, Phys. Rev. D **71**, 043006 (2005).

[9] L. Campanelli, A. D. Dolgov, M. Giannotti, and F. L. Villante, Astrophys. J. **616**, 1 (2004).

[10] C. Scóccola, D. Harari, and S. Mollerach, Phys. Rev. D **70**, 063003 (2004).

[11] M. Pospelov, A. Ritz, and C. Skordis, Phys. Rev. Lett. **103**, 051302 (2009).

[12] A. M. Wolfe, R. A. Jorgenson, T. Robishaw, C. Heiles, and J. X. Prochaska, Nature (London) **455**, 638 (2008).

[13] D. Grasso and H. R. Rubinstein, Phys. Rep. **348**, 163 (2001).

[14] A. P. S. Yadav, L. Pogosian, and T. Vachaspati, arXiv:1207.3356.

[15] L. Pogosian, A. P. S. Yadav, Y.-F. Ng, and T. Vachaspati, Phys. Rev. D **84**, 043530 (2011); Phys. Rev. D **84**, 089903 (2011).

[16] E. Y. S. Wu *et al.* (QUaD Collaboration), Phys. Rev. Lett. **102**, 161 302 (2009).

[17] E. Komatsu, K. M. Smith, J. Dunkley, C. L. Bennett, B. Gold, G. Hinshaw, N. Jarosik, D. Larson, M. R. Nolta, L. Page *et al.*, Astrophys. J. Suppl. Ser. **192**, 18 (2011).

[18] M. Kamionkowski, Phys. Rev. D **82**, 047302 (2010).

[19] E. Komatsu *et al.* (WMAP), Astrophys. J. Suppl. Ser. **180**, 330 (2009).

[20] W. Hu and T. Okamoto, Astrophys. J. **574**, 566 (2002).

[21] M. Kamionkowski, Phys. Rev. Lett. **102**, 111 302 (2009).

[22] A. P. S. Yadav, R. Biswas, M. Su, and M. Zaldarriaga, Phys. Rev. D **79**, 123 009 (2009).

[23] V. Gluscevic, M. Kamionkowski, and A. Cooray, Phys. Rev. D **80**, 023510 (2009).

[24] A. P. S. Yadav, M. Su, and M. Zaldarriaga, Phys. Rev. D **81**, 063512 (2010).

[25] J. Bock, A. Aljabri, A. Amblard, D. Baumann, M. Betoule, T. Chui, L. Colombo, A. Cooray, D. Crumb, P. Day *et al.*, arXiv:0906.1188.

[26] D. Baumann *et al.* (CMBPol Study Team), in *CMBPol Mission Concept Study: Probing Inflation with CMB Polarization*, AIP Conf. Proc. No. 1141 (AIP, New York, 2009).

[27] M. Zaldarriaga, L. Colombo, E. Komatsu, A. Lidz, M. Mortonson, S. P. Oh, E. Pierpaoli, L. Verde, and O. Zahn, arXiv:0811.3918.

[28] K. M. Smith *et al.*, in *CMBPol Mission Concept Study: Gravitational Lensing*, AIP Conf. Proc. No. 1141 (AIP, New York, 2009).

[29] C. Armitage-Caplan, M. Avillez, D. Barbosa, A. Banday, N. Bartolo, R. Battye, J. Bernard, P. de Bernardis, S. Basak *et al.* (The COrE Collaboration), arXiv:1102.2181.

[30] N. J. Miller, M. Shimon, and B. G. Keating, Phys. Rev. D **79**, 103 002 (2009).

[31] B. Keating, S. Moyerman, D. Boettger, J. Edwards, G. Fuller, F. Matsuda, N. Miller, H. Paar, G. Rebeiz, I. Schanning *et al.*, arXiv:1110.2101.

[32] B. R. Johnson, J. Collins, M. E. Abroe, P. A. R. Ade, J. Bock, J. Borrill, A. Boscaleri, P. de Bernardis, S. Hanany, A. H. Jaffe *et al.*, Astrophys. J. **665**, 42 (2007).

[33] B. P. Crill, P. A. R. Ade, D. R. Artusa, R. S. Bhatia, J. J. Bock, A. Boscaleri, P. Cardoni, S. E. Church, K. Coble, P. de Bernardis *et al.*, Astrophys. J. Suppl. Ser. **148**, 527 (2003).

[34] K. W. Yoon, P. A. R. Ade, D. Barkats, J. O. Battle, E. M. Bierman, J. J. Bock, J. A. Brevik, H. C. Chiang, A. Crites, C. D. Dowell *et al.*, in *Society of Photo-Optical Instrumentation Engineers (SPIE) Conference Series* (2006), Vol. 6275 (unpublished).

[35] J. R. Hinderks, P. Ade, J. Bock, M. Bowden, M. L. Brown, G. Cahill, J. E. Carlstrom, P. G. Castro, S. Church, T. Culverhouse *et al.*, Astrophys. J. **692**, 1221 (2009).

[36] W. Hu, M. M. Hedman, and M. Zaldarriaga, Phys. Rev. D **67**, 043004 (2003).

[37] V. Gluscevic, D. Hanson, M. Kamionkowski, and C. M. Hirata, arXiv:1206.5546.

[38] B. Keating, M. Shimon, and A. Yadav (unpublished).

[39] M. Shimon, B. Keating, N. Ponthieu, and E. Hivon, Phys. Rev. D **77**, 083003 (2008).

[40] B. Reichborn-Kjennerud, A. M. Aboobaker, P. Ade, F. Aubin, C. Baccigalupi, C. Bao, J. Borrill, C. Cantalupo, D. Chapman, J. Didier *et al.*, in *Society of Photo-Optical Instrumentation Engineers (SPIE) Conference Series* (2010), Vol. 7741 (unpublished).

[41] J. J. McMahon, K. A. Aird, B. A. Benson, L. E. Bleem, J. Britton, J. E. Carlstrom, C. L. Chang, H. S. Cho, T. de Haan, T. M. Crawford *et al.*, in *American Institute of Physics Conference Series*, edited by B. Young, B. Cabrera, and A. Miller (2009), Vol. 1185, pp. 511–514.

[42] B. P. Crill, P. A. R. Ade, E. S. Battistelli, S. Benton, R. Bihary, J. J. Bock, J. R. Bond, J. Brevik, S. Bryan, C. R. Contaldi *et al.*, in Society of Photo-Optical Instrumentation Engineers (SPIE) Conference Series (2008), Vol. 7010 of Society of Photo-Optical Instrumentation Engineers (SPIE) Conference Series, arXiv:0807.1548.